



3 | Antimicrobial Chemotherapy | Full-Length Text

# Novel hydrazone compounds with broad-spectrum antiplasmodial activity and synergistic interactions with antimalarial drugs

Angélica M. Rosado-Quiñones,<sup>1</sup> Emilee E. Colón-Lorenzo,<sup>1</sup> Zarna Rajeshkumar Pala,<sup>2</sup> Jürgen Bosch,<sup>3,4</sup> Karl Kudyba,<sup>5</sup> Heather Kudyba,<sup>2</sup> Susan E. Leed,<sup>5</sup> Norma Roncal,<sup>5</sup> Abel Baerga-Ortiz,<sup>6</sup> Abiel Roche-Lima,<sup>7</sup> Yamil Gerena,<sup>8</sup> David A. Fidock,<sup>9,10</sup> Alison Roth,<sup>5</sup> Joel Vega-Rodríguez,<sup>2</sup> Adelfa E. Serrano<sup>1</sup>

**AUTHOR AFFILIATIONS** See affiliation list on p. 16.

**ABSTRACT** The development of novel antiplasmodial compounds with broad-spectrum activity against different stages of Plasmodium parasites is crucial to prevent malaria disease and parasite transmission. This study evaluated the antiplasmodial activity of seven novel hydrazone compounds (referred to as CB compounds: CB-27, CB-41, CB-50, CB-53, CB-58, CB-59, and CB-61) against multiple stages of *Plasmodium* parasites. All CB compounds inhibited blood stage proliferation of drug-resistant or sensitive strains of Plasmodium falciparum in the low micromolar to nanomolar range. Interestingly, CB-41 exhibited prophylactic activity against hypnozoites and liver schizonts in Plasmodium cynomolgi, a primate model for Plasmodium vivax. Four CB compounds (CB-27, CB-41, CB-53, and CB-61) inhibited P. falciparum oocyst formation in mosquitoes, and five CB compounds (CB-27, CB-41, CB-53, CB-58, and CB-61) hindered the in vitro development of Plasmodium berghei ookinetes. The CB compounds did not inhibit the activation of P. berghei female and male gametocytes in vitro. Isobologram assays demonstrated synergistic interactions between CB-61 and the FDA-approved antimalarial drugs, clindamycin and halofantrine. Testing of six CB compounds showed no inhibition of Plasmodium glutathione S-transferase as a putative target and no cytotoxicity in HepG2 liver cells. CB compounds are promising candidates for further development as antimalarial drugs against multidrug-resistant parasites, which could also prevent malaria transmission.

**KEYWORDS** malaria, *Plasmodium falciparum*, *Plasmodium berghei*, multistage activity, drug combinations

Malaria continues to be one of the leading causes of death from infectious diseases in endemic areas worldwide, with 247 million cases and 619,000 deaths in 2021 (1). The emergence of multidrug-resistant *Plasmodium falciparum* has significantly worsened the global malaria burden, with increasing incidence and mortality rates (2). Antimalarial monotherapies like chloroquine (CQ) (3–7) and artemisinin (ART) (8–11) have lost their efficacy, prompting the development of novel compounds for combination therapy. The development of new antimalarial drugs is urgently needed to overcome *P. falciparum* resistance and the incidence of malaria.

Malaria is a parasitic protozoan infection caused by *Plasmodium* parasites and transmitted by *Anopheles* mosquitoes. Sporozoites, the infectious stage transmitted by mosquitoes, invade the liver and develop into schizonts, releasing merozoites into the bloodstream. Merozoites invade red blood cells where asexual replication takes place. Some parasites differentiate into gametocytes, which are ingested by mosquitoes when they bite an infected person. The gametocytes form gametes in the mosquito, where

**Editor** Audrey Odom John, The Children's Hospital of Philadelphia, Philadelphia, Pennsylvania, USA

Address correspondence to Adelfa E. Serrano, adelfa.serrano@upr.edu.

Joel Vega-Rodríguez and Adelfa E. Serrano contributed equally to this article.

The authors declare no conflict of interest.

See the funding table on p. 16.

Received 14 December 2023 Accepted 20 March 2024 Published 19 April 2024

Copyright © 2024 Rosado-Quiñones et al. This is an open-access article distributed under the terms of the Creative Commons Attribution 4.0 International license.

they fertilize to form a zygote and then a motile ookinete that invades the midgut epithelium to form an oocyst. The oocyst undergoes sporogony to form sporozoites that invade the mosquito salivary glands. Sporozoites are then transmitted to a new host by a mosquito bite. Historically, antimalarial drugs targeted parasite stages within erythrocytes, neglecting transmission stages in mosquitoes (12). However, liver and mosquito stages represent crucial bottlenecks in the parasite's life cycle, offering the potential for novel transmission-blocking drugs that target multiple stages to interrupt malaria transmission (13).

In searching for new drug targets, we previously identified *Plasmodium* glutathione S-transferase (GST) as an essential erythrocytic protein (14). GST is an important component of cellular detoxification by glutathione conjugation to xenobiotic compounds to increase their solubility and facilitate their excretion from the parasite (15, 16). Using structure-based screening and biological assays, our laboratory previously identified CB-27 as a novel *Plasmodium* GST inhibitor predicted to act at the species-specific H-site (14). Using CB-27 as a query in a shape similarity screening, we also discovered six antiplasmodial compounds (CB-41, CB-50, CB-53, CB-58, CB-59, and CB-61) (14). These CB compounds demonstrated potent antiplasmodial activities *in vitro* against *Plasmodium berghei* intraerythrocytic stages without causing erythrocyte lysis (14).

In this study, we report the antiplasmodial activities of seven CB compounds (CB-27, CB-41, CB-50, CB-53, CB-58, CB-59, and CB-61) against multiple *Plasmodium* stages and species. The compounds were active against *P. falciparum* drug-resistant and drug-sensitive asexual blood stage strains, multiple *Plasmodium* mosquito stages, and liver stages in the *Plasmodium cynomolgi* model. Notably, CB-61 showed synergistic interactions with the FDA-approved antimalarial drugs clindamycin (CLIND) and halofantrine (HALO). Unexpectedly, the six CB compounds did not inhibit their predicted *Plasmodium* GST target. The CB compounds did not demonstrate hepatocytotoxicity. The CB compounds represent a promising advance in developing novel antimalarial candidates as drugs to treat and prevent onward transmission of infection.

#### **RESULTS**

# Plasmodium glutathione S-transferase target inhibition by CB compounds

The inhibition of *Plasmodium* GST by CB compounds (CB-41, CB-50, CB-53, CB-58, CB-59, and CB-61) was assessed by enzymatic inhibition assays using recombinant GST (Fig. 1). Results show that the six CB compounds did not inhibit either *P. falciparum*, *P. berghei*, or human GST (Fig. 1). *Plasmodium* GST inhibition was confirmed by CB-27, which inhibited the activity of recombinant GST from *P. falciparum* (half-maximal inhibitory concentration  $[IC_{50}] = 22.9 \, \mu\text{M}$ ) and *P. berghei* ( $IC_{50} = 21.1 \, \mu\text{M}$ ) but had no activity against human GST. Hemin, used as a positive control, inhibited human ( $IC_{50} = <1 \, \mu\text{M}$ ), *P. falciparum* ( $IC_{50} = 16.1 \, \mu\text{M}$ ) recombinant GST (Fig. S1). These findings suggest that the six CB compounds tested do not target *Plasmodium* GST.

# Antiplasmodial activity of CB compounds: *P. falciparum* blood stages and *P. cynomolgi* liver stages

To determine whether CB compounds inhibit the blood stages of *P. falciparum*, their activities were examined against drug-sensitive (D6) or drug-resistant (TM91c235, W2, and C2B) *P. falciparum* strains. Three resistant strains and one sensitive strain were selected, including TM91c235 (resistant to cycloguanil, pyrimethamine [PYR], mefloquine, sulfadoxine, and quinine, but sensitive to WR99210 and CQ), the Cambodia strain W2 (CQ resistant), the Thai laboratory strain C2B (resistant to atovaquone [ATQ] and sensitive to ART), and the Sierra Leone D6 sensitive strain (17). All CB compounds showed antiplasmodial activity against blood stages of resistant and sensitive strains (Table 1). Interestingly, CB-27 and CB-61 were remarkably active with IC<sub>50</sub> values in the nanomolar range. Overall, these data show that all CB compounds inhibit the blood stages of *P. falciparum*-sensitive and resistant strains.

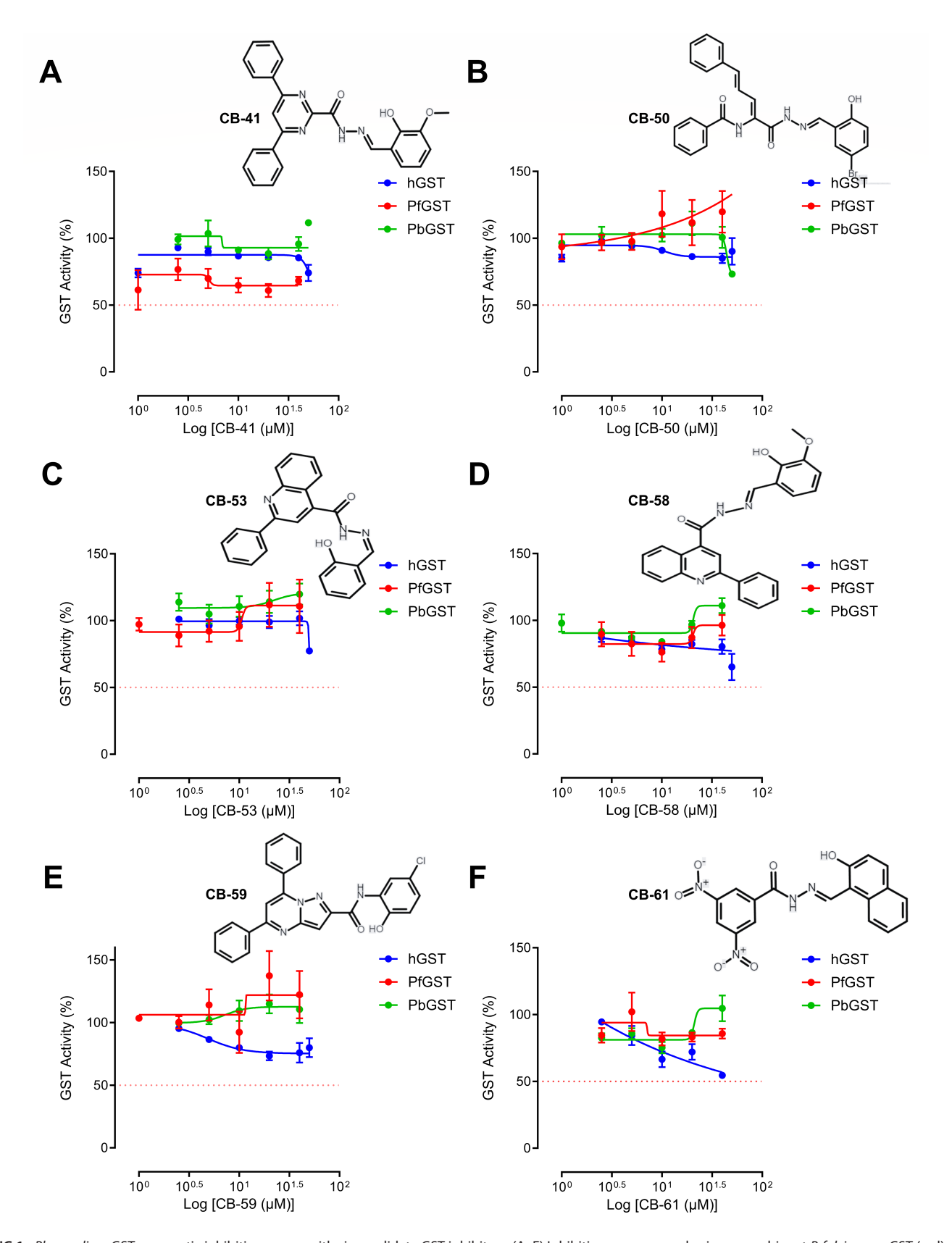


**FIG 1** *Plasmodium* GST enzymatic inhibition assays with six candidate GST inhibitors. (A–F) Inhibition was assessed using recombinant *P. falciparum* GST (red), *P. berghei* GST (green), and human GST (blue) (0.35 mg/mL) in 6-point (1–50  $\mu$ M) dose–response curves. The red dashed lines indicate the 50% inhibition cutoff. To calculate the IC<sub>50</sub> scores, a nonlinear regression function was used for sigmoidal dose–response (variable slope). Positive controls (CB-27 and hemin) are included in Figure S1. Data are presented as mean  $\pm$  SEM from four independent experiments performed in triplicate.

TABLE 1 Antiplasmodial activities of CB compounds in the blood stages of *P. falciparum*-sensitive (D6 and TM91c235) and resistant strains (TM91c235, W2, and C2B)<sup>ab</sup>

	IC <sub>50</sub> (μM) (±SD) for strain:			
Compound	D6	TM91c235	W2	C2B
CB-27	0.28 (±0.19)	0.38 (±0.31)	0.31 (±0.18)	0.40 (±0.24)
CB-41	2.26 (±1.15)	2.26 (±1.10)	2.71 (±1.87)	2.73 (±1.19)
CB-50	1.14 (±0.82)	1.84 (±0.68)	1.15 (±0.59)	1.89 (±1.29)
CB-53	>20	13.89 (±3.56)	>20	>20
CB-58	8.44 (±2.48)	10.62 (±3.05)	5.63 (±2.56)	8.83 (±3.33)
CB-59	1.73 (±1.47)	2.96 (±3.84)	0.69 (±1.08)	2.91 (±1.35)
CB-61	0.20 (±0.05)	0.26 (±0.03)	0.22 (±0.03)	0.30 (±0.12)

<sup>a</sup>Dose–response results are summarized in IC<sub>50</sub> values and standard deviations (SD). These experiments were carried out in two independent experiments performed in triplicate.

<sup>b</sup>P. falciparum strains and sensitivity profiles: D6 = susceptible to CQ, PYR, cycloguanil, and WR99210 (dihydrofolate reductase inhibitor); TM91c235 = susceptible to WR99210 but resistant to cycloguanil, PYR, mefloquine, sulfadoxine, and quinine; W2 = Indochina clone, showing resistance to CQ resistance; C2B = ATQ resistant.

*P. cynomolgi*, a primate malaria model closely related to *Plasmodium vivax*, shares the ability to form dormant liver stages called hypnozoites. These hypnozoites are responsible for recurrent *P. vivax* malaria episodes in humans. We used *in vitro P. cynomolgi* liverstage cultures to investigate the activity of CB compounds (18). Interestingly, CB-41 showed some activity against *P. cynomolgi* hepatic schizonts (IC $_{50}$ : 8.7  $\mu$ M) and hypnozoites (IC $_{50}$ : 8.4  $\mu$ M) stages in the prophylactic drug treatment mode (Table 2). Conversely, CB-41 did not show antiplasmodial activity in the radical cure mode. The remaining six CB compounds did not inhibit the growth of *P. cynomolgi* liver-stage parasites in either the prophylactic or the radical cure mode (Table 2). No hepatocyte toxicity was observed, as evidenced by the preserved viability of primary hepatocytes at concentrations >10  $\mu$ M. The findings suggest that CB-41 could be used to prevent the development and relapse of malaria from the liver stages.

# Antiplasmodial activity of CB compounds: *Plasmodium* gametes, ookinetes, and oocysts stages

To assess the activity of the CB compounds against *P. falciparum* oocyst formation, mosquitoes were fed with infected blood containing mature gametocytes and supplemented with CB compounds in a standard membrane-feeding assay (SMFA). Mosquito midguts were dissected 8 days after feeding to determine the number of oocysts. CB-41 and CB-61 inhibited midgut oocyst formation in a dose-dependent manner, while CB-27 and CB-53 did not (Fig. 2A through D; Tables S 2–S3). Although CB-41 statistically inhibited oocyst formation compared to the control, its median and prevalence inhibition percentages were below 50% (Fig. 2B; Table S2-S3), indicating weak activity against oocysts. The results show that CB compounds CB-50 and CB-58 did not inhibit oocyst formation (Fig. 2E and F;Table S2–S3).

CB compound activity against *P. berghei* ookinete development was measured *in vitro* using the luminescence signal from Ookluc parasites. As Ookluc expresses luciferase

**TABLE 2** Prophylactic antiplasmodial activity of CB-41 in hypnozoites and hepatic schizonts in the *P. cynomolgi* model<sup>a</sup>

Compound	Toxicity (μM)	Hypnozoite IC <sub>50</sub> (μM)	Schizont IC <sub>50</sub> (μM)	Total parasite IC <sub>50</sub> (μM)
CB-27	>10	>10	>10	>10
CB-41	>10	8.7	8.4	8.6
CB-50	>10	>10	>10	>10
CB-53	>10	>10	>10	>10
CB-58	>10	>10	>10	>10
CB-59	>10	>10	>10	>10
CB-61	>10	>10	>10	>10

These experiments were performed in one independent experiment, triplicate for the prophylactic drug treatment mode, and duplicate for the radical cure mode.

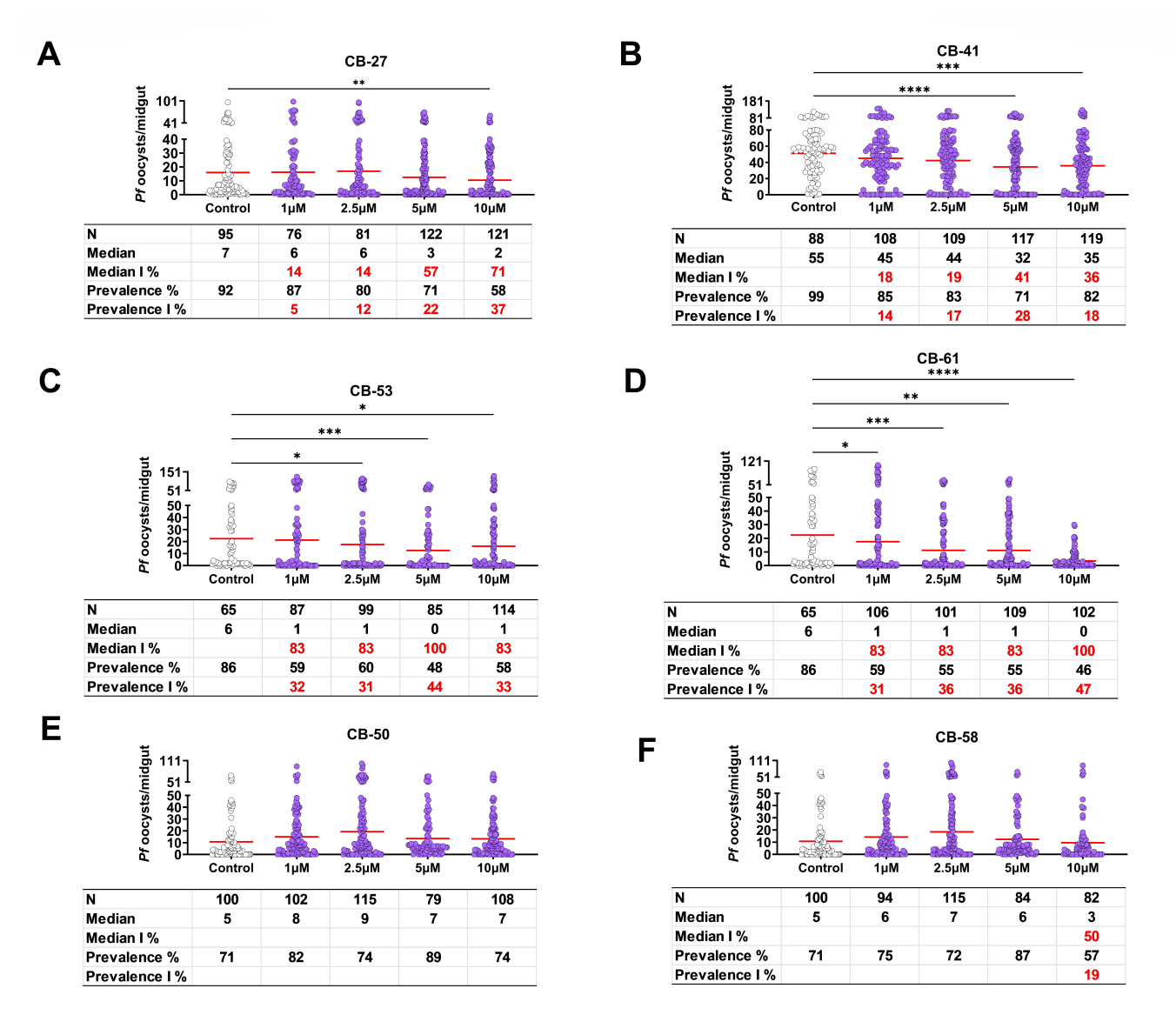


FIG 2 Antiplasmodial activity of CB compounds on *P. falciparum* oocyst formation. *Anopheles stephensi* mosquitoes were fed with *P. falciparum* infectious blood supplemented with increasing concentrations (1 to 10 μM) of the CB compounds or DMSO control using SMFA. Horizontal red lines represent the median. Data were pooled from two representative experiments. Additional experiments are shown in Table S2. Statistical analysis was performed using the Kruskal-Wallis test with the Dunn post-test. \*P < 0.021, \*\*P < 0.0021, \*\*\*P < 0.00021, and \*\*\*\*P < 0.000021. Median I%, median inhibition percentage; N, number of mosquitoes dissected; median I% or prevalence I%: 100 × ([number of positives in control – number of positives in experimental]/[number of oocysts in control]). (A) CB-27, (B) CB-41, (C) CB-53, (D) CB-61, (E) CB-50, (F) CB-58.

under the ookinete-specific *ctrp* promoter, luminescence directly reflects the ookinete number. Dose–response curves with 6-point concentrations were generated for each CB compound. Results demonstrate that five CB antiplasmodial compounds (CB-27, CB-41, CB-53, CB-58, and CB-61) inhibit ookinete development (Fig. 3A through G). CB-27 exhibited the lowest IC50 (9.2  $\mu$ M) of the CB compounds, followed by CB-53 (14.7  $\mu$ M), CB-41 (16.6  $\mu$ M), CB-61 (29.5  $\mu$ M), and CB-58 (32.5  $\mu$ M). CB-50 and CB-59 showed no activity in ookinete formation (Fig. 3C and F). These results demonstrated that five CB compounds inhibit *P. berghei* ookinete *in vitro* development, suggesting that CB compounds act in the *Plasmodium* mosquito stages after fertilization.

The activity of CB compounds was evaluated for inhibition of P. berghei male and female gamete activation. Male gamete activation was assessed by inducing exflagellation in the presence of each CB compound at 10  $\mu$ M for 15 minutes and counting

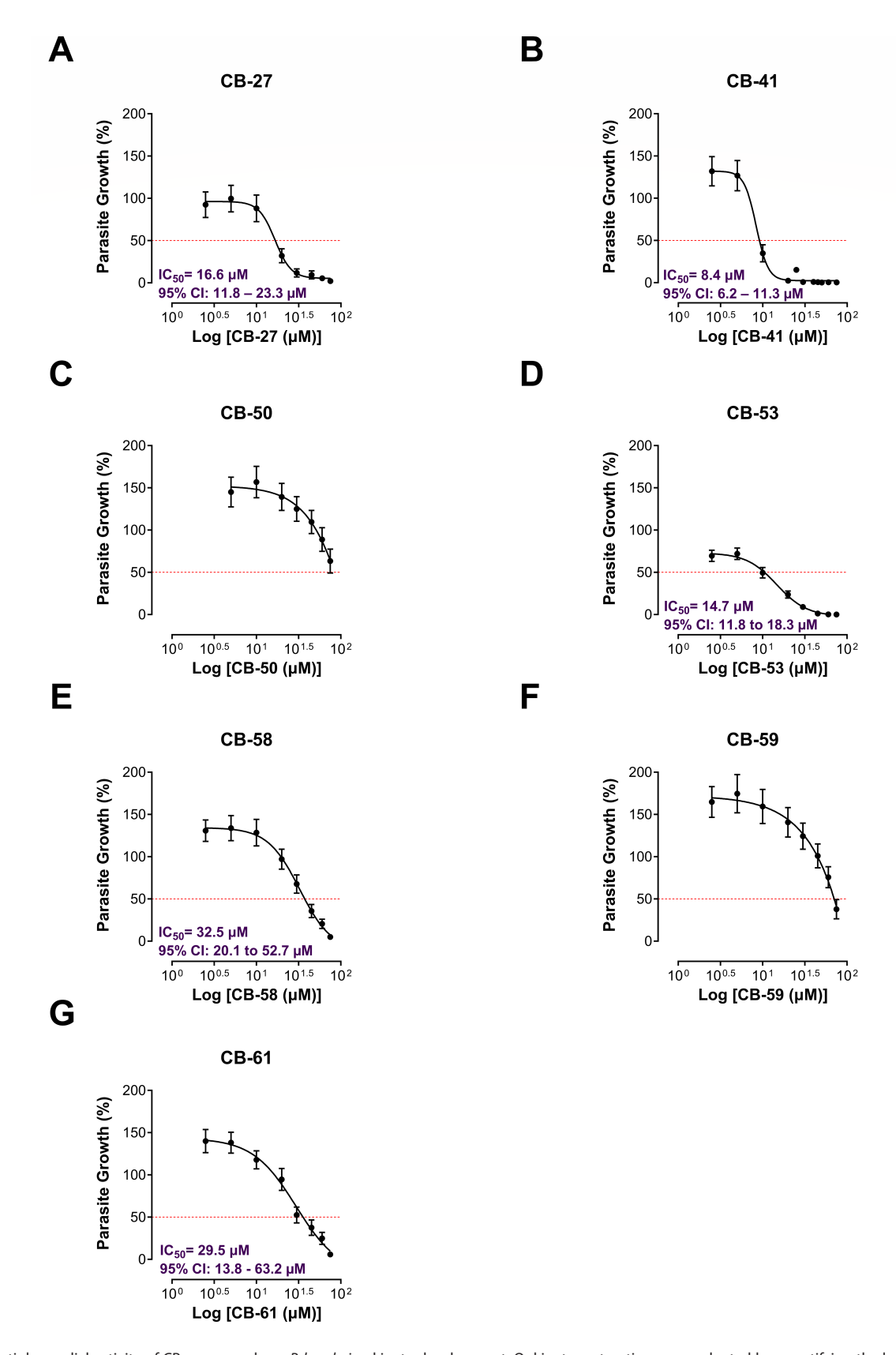


FIG 3 Antiplasmodial activity of CB compounds on *P. berghei* ookinete development. Ookinete maturation was evaluated by quantifying the luciferase activity expressed by Ookluc parasites, which harbor the luciferase gene driven by the ookinete-specific *ctrp* gene promoter. The red dashed lines indicate the 50% inhibition cutoff. To calculate the IC<sub>50</sub> scores, a nonlinear regression function was used for sigmoidal dose–response (variable slope). Data are presented as mean  $\pm$  SEM and represent three independent experiments each performed in triplicate. (A) CB-27, (B) CB-41, (C) CB-50, (D), CB-53, (E) CB-58, (F) CB-59,(G) CB-61.

exflagellations by microscopy (Fig. 4A). The results revealed that none of the CB compounds affected *P. berghei* exflagellations, while aphidicolin, a DNA polymerase inhibitor used as a positive control, showed a significant reduction in the number of exflagellation events (<50%) (Fig. 4A). To determine their activity against female gamete activation, infected blood was incubated with 10 µM of each CB compound for 2 hours and then analyzed by flow cytometry. The macrogamete subpopulation was identified by staining with antibodies against the surface marker Pbs21, which is only produced in activated female gametes and zygotes (Fig. 4C through E). The CB compounds did not inhibit the activation of *P. berghei* female gametes (Fig. 4B). Collectively, these data demonstrated that CB compounds do not affect male and female gamete activation. These results indicate that CB-27, CB-41, CB-53, and CB-61 inhibit the development of oocysts in the mosquito midgut, representing potential transmission-blocking antiplasmodial drugs.

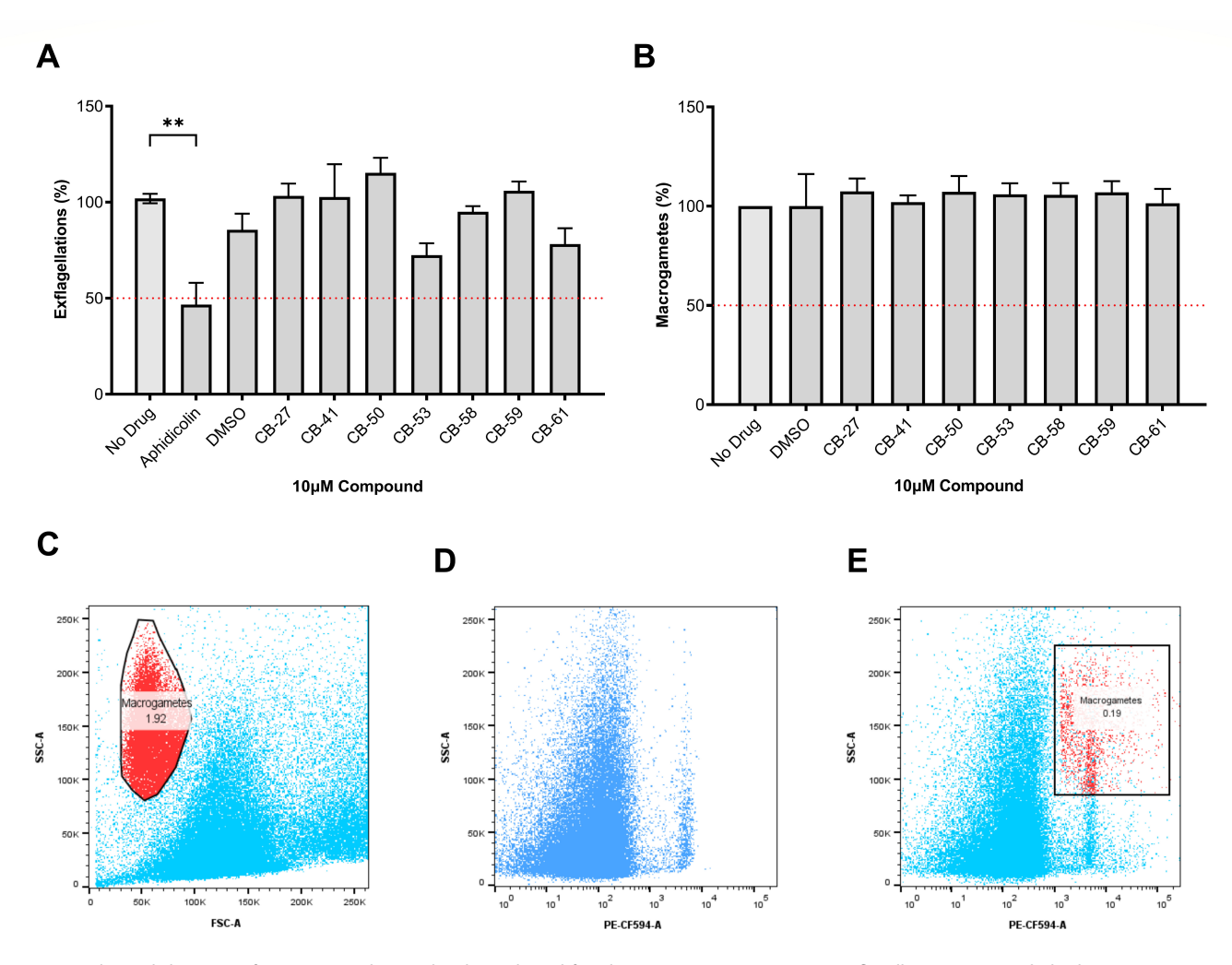


FIG 4 Antiplasmodial activity of CB compounds on *P. berghei* male and female gametocyte activation. (A) Exflagellation assays. Aphidicolin (125 nM), a DNA polymerase inhibitor, was a positive control to block exflagellations (19). (B) Macrogamete flow cytometry assays were carried out to determine *in vitro* inhibition of CB compounds on female gametocyte activation. Female gametes were detected by staining with antibodies against the surface protein Pbs21. The red dashed lines indicate the 50% inhibition cutoff. Data are presented as mean ± SEM and represent three independent experiments performed in triplicate. Statistical analysis was conducted using one-way ANOVA with Dunnett's multiple comparison tests. The significance level was \*\*P < 0.0021. (C–E) Gating strategy for flow cytometry analysis of *P. berghei* macrogametes (red – %) labeled with anti-Pbs21 antibody and Alexa Fluor 594 secondary antibody from a pool of red blood cells and immune cells (blue). (C) Side (SCC-A) and forward scatter area (FSC-A) dot plot of *P. berghei* macrogametes in culture. (D) SSC-A vs PE-CF594 dot plot of *P. berghei* macrogametes in culture with both antibodies.

TABLE 3 Cytotoxicity and SI of CB compounds in the mammalian HepG2 hepatoma cell line<sup>b</sup>

Compound	HepG2 cytotox (μM)	SI (relative to WR288510-3°)
CB-27	>20	>100-fold
CB-41	>20	>100-fold
CB-50	>20	>100-fold
CB-53	>20	>100-fold
CB-58	>20	>100-fold
CB-59	>20	>100-fold
CB-61	>20	>100-fold
WR288510-3 <sup>a</sup>	1.28	1-fold

<sup>&</sup>lt;sup>a</sup>Positive control.

# In vitro cytotoxicity of CB compounds in HepG2 cells

A counter-screen with uninfected HepG2 mammalian cells was performed to assess the potential cytotoxicity and selectivity index (SI) of CB compounds (CB-27, CB-41, CB-50, CB-53, CB-58, CB-59, and CB-61) in human liver cells. No hepatotoxicity of the CB compounds was observed at the highest concentration tested (20.2  $\mu$ M) in HepG2 hepatoma cells when compared to the IC<sub>50</sub> of the positive control WR288510-3 (1.3  $\mu$ M) (UPSOT 7259167B2) (Table 3). The SI (20, 21), a decisive metric signifying the antimalarial selectivity of the CB compounds in relation to the positive control WR288510-3, exceeds the 100-fold threshold (Table 3). These findings suggest that the CB compounds did not induce host hepatotoxicity.

# Antiplasmodial synergistic interactions: CB-61 and FDA-approved antimalarial drugs

Synergistic combinations between CB-61 and 85 FDA-approved antimalarial drugs were predicted using the Machine Learning Synergy Predictor tool (MLSyPred) (22). Five potential synergistic combinations were predicted (Fig. S2), and isobolograms were used to validate antiplasmodial synergistic predictions in P. berghei blood stages. The synergistic antimalarial drugs predicted were ATQ, CLIND, dihydroartemisinin (DHA), HALO, and lumefantrine (LUM). Isobologram analyses show the interactions of the drug combinations in terms of synergism, additive, and antagonism. In the isobologram, points located significantly below the line connecting the half-maximal fractional inhibitory concentration (FIC<sub>50</sub>) of 1 from both compounds (diagonal black line) indicate a synergistic interaction, while points close to the line suggest an additive interaction. Conversely, points well above the line signify an antagonistic interaction. Results showed that CB-61 displayed antiplasmodial synergistic interactions with CLIND and HALO (Fig. 5A). In contrast, antagonistic interactions were detected between CB-61 and ATQ, DHA, and LUM (Fig. 5A). As predicted, the positive control combination (LUM-DHA) exhibited synergy, whereas the negative control combination (CB-61 and CQ) showed antagonism (Fig. 5B). The results are shown as the mean of the sums of the FIC50 values per combination (mean  $\Sigma FIC_{50}$ ) and are represented in heatmaps (Fig. 5C). The precision of the MLSyPred tool was improved to 57%, potentially representing a valuable tool for predicting the synergistic combinations of antimalarial drugs (Table 4). The findings suggest that CB-61 has the potential to be a synergistic partner with select antimalarial drugs.

### **DISCUSSION**

The development of novel antimalarial drugs with activity against the multiple stages of the *Plasmodium* parasite is crucial to combating multidrug-resistant parasites and preventing malaria transmission. New antimalarial drugs that target different *Plasmodium* species stages can improve treatment efficacy, reduce the risk of resistance

<sup>&</sup>lt;sup>b</sup>Data represent two independent experiments.

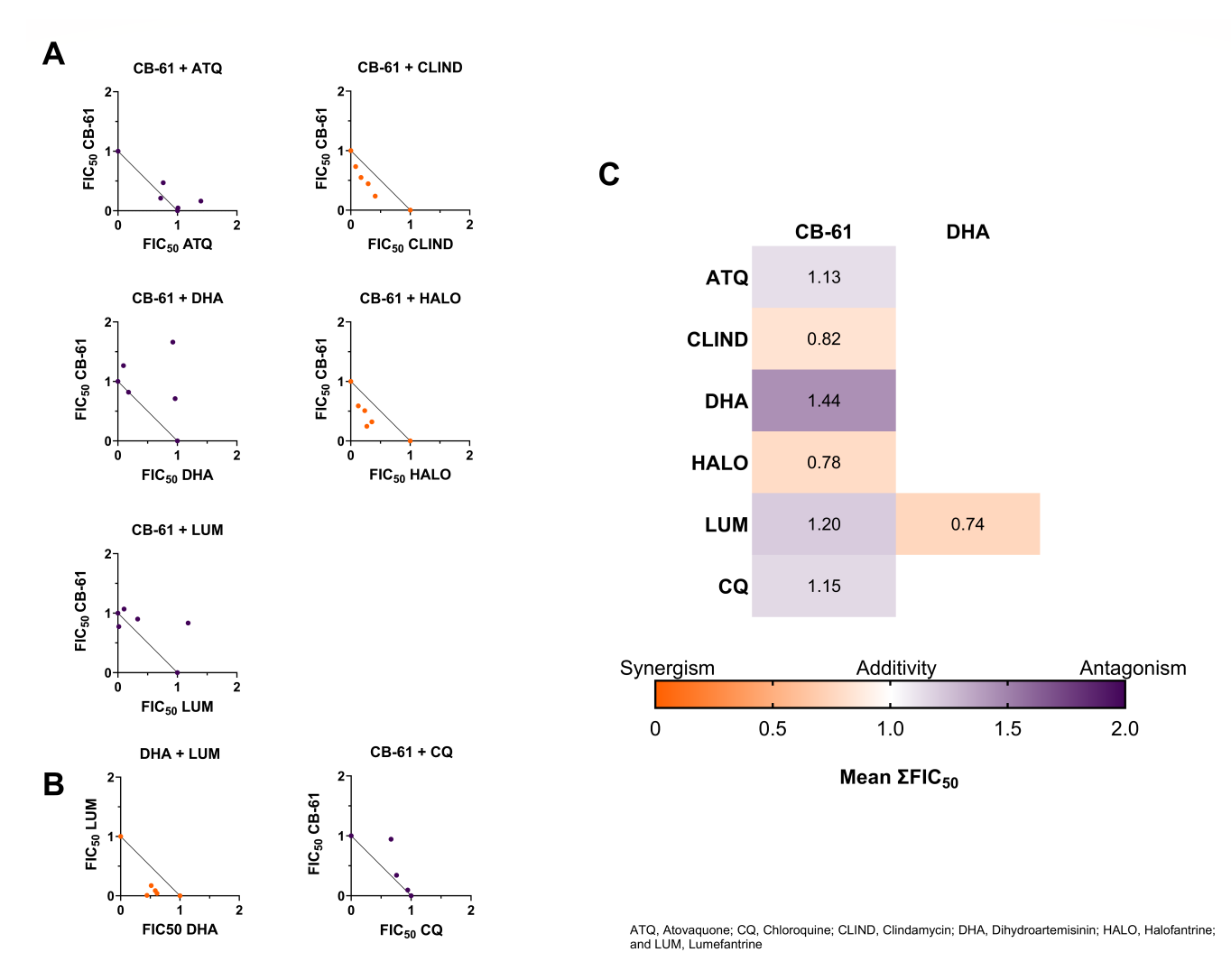


FIG 5 Isobolograms of drug combinations of CB-61 with FDA-approved antimalarial drugs. (A) Isobolograms of CB-61 with ATQ, CLIND, DHA, HALO, and LUM. (B) Isobolograms of positive and negative controls. The *P. berghei* blood-stage parasites were exposed to drug combinations in fixed ratios of their IC<sub>50</sub> scores (5:0, 4:1, 3:2, 2:3, 1:4, 0:5). FIC<sub>50</sub> values were plotted for each drug combination and the fixed ratio. The results were compared against a full black line representing the perfect additive trend (1,1). The classifiers used were synergy FIC<sub>50</sub> < 1 (orange); additivity FIC<sub>50</sub> = 1 (white); and antagonism FIC<sub>50</sub> > 1 (purple). (C) Heatmaps of the means of the sum of FIC<sub>50</sub> ( $\Sigma$ FIC<sub>50</sub>) of the five experimental and the two control combinations. LUM-DHA is a proven synergistic combination (positive control), and CB-61-CQ displays an antagonistic interaction (negative control). Data are presented as means of the sums of the FIC<sub>50</sub> scores and represent three independent experiments performed in triplicate. ATQ, atovaquone; CQ, chloroquine; CLIND, clindamycin; DHA, dihydroartemisinin; HALO, halofantrine; and LUM, lumefantrine.

development, and potentially eliminate the parasite from both humans and mosquitoes. Our previous work identified CB-27, a specific inhibitor of *P. berghei* GST, active in *P. falciparum*, and six additional CB compounds that inhibit *P. berghei* erythrocytic stages (14). Herein, we report the broad-spectrum activity of the seven novel antiplasmodial CB compounds (CB-27, CB-41, CB-50, CB-53, CB-58, CB-59, and CB-61) on blood, liver, and mosquito stages of *Plasmodium* species parasites. The potential for synergistic interactions in combinatorial therapy was demonstrated. Our results reveal that the CB compounds are promising new candidates for the development of multistage antimalarial drugs.

The CB compounds were selected *in silico* to target the *Plasmodium* GST. The identified CB-27 compound was predicted and demonstrated to inhibit *Plasmodium* GST (14), an attractive target because it is directly involved in detoxifying reactive oxygen species (15, 16). Our previous work has shown that *Plasmodium* 

**TABLE 4** Machine learning predictions obtained by MLSyPred, an open-source tool to predict synergistic antimalarial drug combinations and their subsequent validation using *P. berghei* isobolograms

Compound	Compound	Prediction	Validation
CB-61	ATQ	Synergy	Antagonism
CB-61	CLIND	Synergy	Synergy
CB-61	DHA	Synergy	Antagonism
CB-61	HALO	Synergy	Synergy
CB-61	LUM	Synergy	Antagonism
CB-61	CQ	No synergy	Antagonism
LUM <sup>a</sup>	$DHA^a$	Synergy	Synergy

<sup>&</sup>lt;sup>a</sup>Positive control; a proven synergistic interaction (23).

gamma-glutamylcysteine synthetase and glutathione reductase are critical for mosquitostage survival, and the *Plasmodium* cytosolic GST is an essential protein in blood-stage parasites, representing a good target for the development of novel compounds (14, 16, 20–22).

In a previous study, our laboratory identified six CB compounds by shape similarity screening using CB-27, a Plasmodium GST inhibitor, as a query. The identified CB-27 compound was predicted and demonstrated to inhibit Plasmodium GST (14). Our results, however, show no inhibition of Plasmodium GST by the six CB compounds analyzed. Nonetheless, all CB compounds exhibited multistage and multispecies *Plasmodium* inhibition, suggesting they target other proteins or pathways essential for Plasmodium species survival. The discrepancy between predicted and validated inhibition of Plasmodium GST by the six CB compounds likely arises from the Rapid Overlay of Chemical Structures (ROCS) similarity score limitations. Although ROCS scores assess similarity to known inhibitors based on binding affinity, toxicity, and other properties, they have been shown to be inaccurate for some compounds (18, 24-26). Studies on HIV-1 proteases and phosphoinositide 3 kinase delta identified few molecules exhibiting inhibitory activity and low IC50 values despite high ROCS scores, suggesting that shape similarity alone may not be sufficient for accurate prediction (25, 26). Specific inhibitor tools utilizing large data sets and focusing on shared structural features and binding affinities could offer a more practical approach to identifying potent inhibitors (18, 24-27).

Despite the limitations of ROCS similarity screening, we discovered CB-27 as a putative *Plasmodium* GST inhibitor (14). CB-27 differs in structure and mode of action from known GST inhibitors such as hemin and S-hexylglutathione. Hemin, an iron-containing porphyrin derived from heme, binds the GST G-site, inhibiting glutathione conjugation due to its planar structure (28–33). Meanwhile, S-hexylglutathione, a hexyl chloride glutathione conjugate, binds both G and H sites with its non-planar structure, further enhancing inhibition (28, 29, 33, 34). The *Plasmodium* GST inhibitor CB-27 is a hydrazone compound predicted to bind the *Plasmodium* species-specific H-site without affecting the evolutionary preserved G-site (14, 35). In this study, we further validated the inhibition of *Plasmodium* GST by CB-27 using recombinant proteins, specifically by measuring the enzymatic activity of recombinant *Plasmodium* GST. Further studies are needed to determine the target pathway of the remaining CB compounds and optimize their properties for preclinical development.

This study investigated the activity of the CB compounds against the blood stages of *P. falciparum*-resistant and sensitive strains. Our results revealed that all seven CB compounds inhibited the growth of *P. falciparum* blood stages in all four strains tested. The most potent inhibitors were CB-27 and CB-61, which inhibited parasite growth at nanomolar concentrations in all strains. Further research on CB compounds will be needed to determine whether or not the parasite can develop resistance to these drugs. Our findings suggest that CB compounds, especially CB-27 and CB-61, represent promising antiplasmodial candidates that can clear asexual blood-stage parasitemia.

Inhibition of both liver schizonts and hypnozoites is an important attribute of CB-41. *P. vivax* and *Plasmodium ovale* are the only human malaria parasites with hypnozoite stages, which can persist in hepatocytes and cause relapse of infection days, weeks, months, and years after the end of drug treatment (36, 37). Both primaquine and tafenoquine are 8-aminoquinoline drugs approved by the FDA against anti-hepatic schizonts and hypnozoites, which prevent *P. vivax* relapse (38–40). Unfortunately, primaquine is underused worldwide as it can cause hemolytic anemia in individuals with low glucose-6-phosphate dehydrogenase activity. Safer treatments are urgently required (41). Identifying novel compounds active against hypnozoites and liver-stage schizonts in *Plasmodium* relapsing models is crucial to malaria eradication. Most recently, other novel *P. vivax* hypnozoite and hepatic schizont inhibitors have reported IC<sub>50</sub> values under 10 µM, but none were tested in multiple *Plasmodium* species and stages (42, 43). Structural modification of CB-41 can help improve its activity. CB-41 is our first compound to initially show activity against both *P. cynomolgi* liver schizonts and hypnozoites *in vitro*.

Primaquine is the only licensed antimalarial drug recommended by WHO that kills late-stage gametocytes and prevents *P. vivax* relapse (39). In this study, we evaluated the activity of CB compounds in blood gametocytes and transmission stages in the mosquito host. CB-27, CB-41, CB-53, and CB-61 inhibited oocyst formation in mosquitoes, thus possessing the criteria to block transmission stages. We also observed that CB-27, CB-41, CB-53, CB-58, and CB-61 blocked *P. berghei* ookinete development in a dose-dependent manner. The CB compounds did not affect *P. berghei* micro- and macro-gamete formation when incubated with gametocytes at the moment of the assay. Our data show that CB compounds are active against mosquito stages after fertilization during ookinete and oocyst formation.

Determining the pharmacokinetics and toxicity of a compound is a crucial step in the early stages of drug development because this information can be used to prioritize promising drug candidates and optimize the development of lead compounds (44). Previously, we showed that the CB compounds do not induce hemolysis of erythrocytes (14). The CB compounds demonstrated no toxicity in mammalian cells, as evidenced by their lack of cytotoxicity against the HepG2 hepatoma cell line at concentrations up to 20.2 µM. Similarly, no toxicity was observed in primary hepatocytes in the *P. cynomolgi* liver-stage assays. Previous ADMET (Absorption, Distribution, Metabolism, Excretion, Toxicity) predictions revealed that CB compounds had hepatoxicity similar to CQ (14). Further studies are needed to evaluate the potential long-term effects of CB compounds on host cells prior to preclinical testing.

Combination therapy has been central to preventing resistance against the few antimalarial drugs available. In this study, we explored potential partner drugs for CB-61 combination therapies. In this study, 85 antimalarial drugs were selected and tested for synergistic interactions with CB-61. Drug combinations can display three primary types of interactions: synergism, additivity, and antagonism. Synergism occurs when the combined effect of two or more drugs exceeds the sum of their actions, leading to enhanced therapeutic outcomes and potentially reduced drug dosages (45-48). Additivity signifies that the combined effect of drugs is similar to the sum of their individual actions, neither enhancing nor diminishing each other's actions. This neutral interaction is represented by the additive (1,1) line in isobologram graphs (46). In contrast, antagonism arises when the combined effect of two or more drugs is less than the sum of their actions, causing a weakened therapeutic response (46). Fixed-ratio isobologram studies revealed synergy between CB-61 and two antimalarial drugs: CLIND and HALO. CLIND is a repurposed drug that binds to the 50s bacterial ribosomal subunit, disrupting protein synthesis (49). Meanwhile, HALO hinders the polymerization of heme molecules, and the parasite is poisoned with its waste products (50). These structurally diverse drugs have different mechanisms of action that can work in unison with CB-61, thus creating synergy. The synergistic drug interactions of CB-61 make it an attractive

candidate for combination therapies that can clear the pathogenic asexual blood stages and prevent transmission.

We report here a series of CB compounds (CB-27, CB-41, CB-50, CB-53, CB 58, CB-59, and CB-61) that are lead candidates for further investigation as broad-spectrum antimalarial drugs. Our results revealed greater efficacy against drug-resistant and sensitive *Plasmodium* blood stages. Remarkably, the CB compounds also exhibit antiplasmodial activity against mosquito and liver stages, emerging as promising therapeutic leads for malaria.

#### **MATERIALS AND METHODS**

#### Parasites, cell lines, antibodies, and reagents

P. berghei GFP-Lucama1, expressing the green fluorescent protein and firefly luciferase genes under the control of the ama-1 schizont-specific promoter, was provided by the Leiden University Malaria Research Group and was utilized for isobologram experiments (51). Similarly, P. berghei Ookluc, expressing luciferase under the P. berghei circumsporozoite protein and thrombospondin-related adhesive protein (CTRP) promoter, was obtained from Daniel Bargieri and Richard Eastman from the NIH and was employed in experiments involving macrogametes, microgametes, and ookinetes (52). Maintenance of mosquitoes and P. falciparum was performed as previously described (53). Laboratory strains of P. falciparum (D6, TM91-C235, W2, and C2B) were maintained and used for in vitro Malaria SYBR Green I-Based Fluorescence (MSF) assays. The Anopheles dirus mosquitoes harboring *P. cynomolgi bastianellii* (B strain) sporozoites were used to infect the primary primate hepatocytes, which were obtained cryopreserved from BioIVT Inc. (Baltimore, MD, USA) and maintained in hepatocyte culture medium (HCM) (InVitroGro CP medium). Recombinant GST proteins from P. falciparum (PfGST), P. berghei (PbGST), and human (hGST) were obtained from InterRayBio, LLC (Cleaveland, OH, USA) and were utilized for GST inhibition assays. The CB compounds (CB-27, CB-41, CB-50, CB-53, CB-58, CB-59, and CB-61) were obtained from the ChemBridge Hit2lead library (San Diego, CA, USA). The anti-Pbs21 mouse monoclonal antibody, prepared in Joel Vega-Rodríguez laboratory at the NIH, and anti-mouse goat IgG conjugated Alexa Fluor 594, from Invitrogen, were used in immunofluorescence assays. Human hepatocarcinoma cells (HepG2) were cultured in complete Minimal Essential Medium (MEM) (Gibco-Invitrogen, #11090-099) supplemented with 0.19% sodium bicarbonate (Gibco-BRL), 10% heat-inactivated fetal bovine serum (Gibco-Invitrogen), 2 mM L-glutamine (Gibco-Invitrogen), 0.1 mM MEM nonessential amino acids (Gibco-Invitrogen), 0.009 mg/mL insulin, and 1.76 mg/mL bovine serum albumin. All reagents, unless otherwise stated, were purchased through Sigma (St. Louis, MO, USA).

# **GST** plasmid constructs

The open reading frames encoding PfGST, PbGST, and hGST were gene-synthesized and harmonized from their respective genomic DNA using sequence-specific sense oligonucleotides (Table S1). The sequences, produced as a geneblock by Integrated DNA Technologies Inc., were cloned into the *Escherichia coli pRSF-1b* expression vector with a KanR cassette. All recombinant proteins were codon-optimized for bacterial expression using JCat (54). The antisense oligonucleotide encoded a His10 tag for purification (HisTrap excel Ni Sepharose, Cytiva), a Tobacco Etch Virus cleavage site, and an Avitag with one lysine for biotinylation or streptavidin purification/surface plasmon resonance chip binding. The PfGST, PbGST, and hGST constructs consisted of 247, 241, and 258 amino acids with molecular weights of ~29.3, ~28.5, and ~30.1 kDa, respectively.

# **GST** expression and purification

Recombinant GST proteins were produced from frozen E. coli BL21 (DE3) cultures in Terrific Broth with kanamycin for 16 hours. Induction was triggered with isopropyl β-D-1-thiogalactopyranoside at OD600 3.0, followed by centrifugation (1,000  $\times$  g for 15 minutes at 25°C) and pellet freezing at -20°C. Pellets were resuspended in BugBuster, protein inhibitor cocktail, and benzonase nuclease, followed by 20 minutes of incubation and removal of insoluble cell debris by centrifugation (35 minutes at 12,000  $\times$  g at 4°C). GST proteins were purified by affinity chromatography using a HisTrap Excel Ni Sepharose column and an ÄKTA Go system (Cytiva) at a 1-mg/mL flow rate. The column was washed with distilled water and then sequentially with equilibration buffer (1 M phosphate buffer, 1 M NaCl, pH 7.4), protein lysate, wash buffer (25 mM Tris, 500 mM NaCl, 20 mM imidazole, 1 mM DTT), and elution buffer (500 mM imidazole, 20 mM sodium phosphate monobasic, 0.5 M NaCl, 1 mM DTT). Finally, the column was washed and prepared with distilled water and 20% ethanol. Western blot analysis confirmed the presence of the three GST proteins (1:1,000 PentaHis HRP Antibody, LI-COR Western-Sure PREMIUM chemiluminescence). Pooled fractions containing GST proteins were concentrated using a 5-kDa cutoff polyethersulfone tube (1,000  $\times$  g, 3 cycles, 90 min/ cycle) and were adjusted to pH 7.4.

# **GST** inhibition assay

Enzymatic activities of recombinant GSTs were determined spectrophotometrically using the chromogenic substrate 1-chloro-2,4-dinitrobenzene (CDNB). Recombinant GST (0.35 mg/mL) was mixed with 1 mM CDNB in 100 mM HEPES. Stock solutions (10 mM) of the CB compounds and hemin were prepared in 100% dimethyl sulfoxide (DMSO) and then diluted at 0.5% DMSO (14). Each inhibitor has six concentrations ranging from 1 to 50  $\mu$ M. The reaction was initiated with 1 mM glutathione (GSH) after 15 minutes. Absorbance change at 340 nm was measured for 1 hour. The slope was converted to micromole per minute using Beer's equation and the extinction coefficient for the product S-(2,4-dinitrophenyl)glutathione ( $\epsilon$ 340 nm = 9.6 mM $^{-1}$  cm $^{-1}$ ) (14). The assay was validated using human placenta GST (#G8642) as a positive control.

#### P. falciparum SYBR Green drug sensitivity assessment

MSF assays were performed *in vitro* with four *P. falciparum* strains: D6 (drug sensitive), TM91-C235 (multidrug resistant), W2 (CQ resistant), and C2B (multidrug resistant against ATQ). Parasite strains were kept continuously in long-term cultures as described (22). Pre-dosed 384-well plates containing 12-fold serial dilutions of CB compounds (0.0098–20 μM) were prepared using the Tecan Freedom Evo liquid handling system (Tecan USA, Inc., Durham, NC, USA) and were stored at 4°C. A CQ control plate (2,000 ng/mL) was included in each run. Based on modifications of previous methods (17, 55), late-ring or early-trophozoite stages were cultured in pre-dosed plates with 0.3% parasitemia and 2% hematocrit. Cultures were incubated for 72 hours at 37°C in a controlled atmosphere of 5% CO<sub>2</sub>, 5% O<sub>2</sub>, and 90% N<sub>2</sub>. Lysis buffer, consisting of 20 mM Tris HCl, 5 mM EDTA, 1.6% Triton X, 0.016% saponin, and SYBR Green I dye at a 20X concentration (Invitrogen #S-7567), was added to the plates for a final 10X SYBR Green concentration. Plates containing cell culture media and lysis buffer were incubated in the dark at 25°C for 24 hours, and the relative fluorescence units (RFU) were measured using the Tecan Genios Plus (Tecan USA, Inc.).

# P. cynomolgi liver-stage inhibition assay

Primary primate hepatocytes were seeded in 384-well plates and used within 2–4 days (56). *P. cynomolgi* B strain parasites were inoculated and developed into hypnozoites and schizonts. CB compounds were tested in 8-point, threefold serial dilutions (100  $\mu$ M to 5 nM) for both prophylactic (4 days starting with sporozoite addition) and radical cure (4 days starting day 4 post-inoculation) modalities (56–60). The Operetta CLS imaging

system and Harmony Software 4.9 (Perkin Elmer, Waltham, MA, USA) analyzed the plates, and the percentage of inhibition (PI) was calculated in Python using equation (1), where parasitic quantities (hypnozoite and schizont counts) were normalized to the negative control (57). Each plate included negative (DMSO) and positive (KDU691, maduramicin, tafenoquine) controls (58). IC<sub>50</sub> values were determined using an 8-point, threefold dilution format and a Python-adapted grid algorithm for fitting PI to a four-parameter logistic function (61).

Equation (1) Percent inhibition

$$PI = 100 * \left(1 - \left(\frac{xy}{Mean^{neg}}\right)\right)$$

### P. falciparum oocyst inhibition assay

As previously described, *P. falciparum* infections were performed using SMFA with NF54 gametocyte cultures diluted to 0.3% stage V gametocytemia (62). Infected blood (O+human 45% hematocrit in serum) was offered to mosquitoes for 30 minutes, and engorged mosquitoes were maintained on a 10% corn syrup solution supplemented by four concentrations of CB compounds (1, 2.5, 5, and 10  $\mu$ M) at 37°C (63), with DMSO serving as a control. Eight days post-infection, mosquito midguts were dissected and stained with 0.2% mercurochrome for 30 minutes, and oocysts were quantified under a light microscope (63).

# P. berghei ookinete luciferase inhibition assay

Mice were pretreated with phenylhydrazine [6 mg/mL, intraperitoneal injection (IP)] 3 days before intravenous injection (IV) infection with *P. berghei* Ookluc parasites (19, 62). Once parasitemia exceeded 15%, the mice received PYR (1 mg/mL, IP) (19, 62). Twenty-four hours after PYR treatment, infected mice were assessed for at least 10 exflagellations before blood was collected by heart puncture (19, 62). Infected blood (1:20 dilution) was incubated with 8-point serial dilutions (2.5–75  $\mu$ M) of CB compounds for 24 hours at 19°C with gentle shaking (62, 64). Relative luminescence units (RLU) of mature ookinetes were measured using the Promega Nano-Glo Luciferase Assay System Kit and a SpectraMax M3 Microplate Reader (Molecular Devices, San Jose, CA, USA) after 3 minutes. Giemsa blood smears confirmed ookinetes.

#### P. berghei gametocyte activation assays

Exflagellation assays were performed to assess the effect of CB compounds on *P. berghei* male gametocyte activation (19). Tail blood from PYR-administered mice was mixed with DMSO, aphidicolin (125 nM), or CB compounds (10  $\mu$ M) in complete ookinete medium and heparin (30  $\mu$ g/mL) (19). After a 15-minute incubation, the sample was diluted in complete ookinete medium with 10  $\mu$ M inhibitor and adjusted to a final blood concentration of 1:20. Exflagellations were quantified by counting all events in the middle squares of a hemocytometer. The effect of CB compounds on macrogamete formation was analyzed by flow cytometry using the anti-Pbs21 antibody (65). Following PYR administration, infected blood for cardiac puncture was cultured with CB compounds (10  $\mu$ M) for 2 hours to stimulate gametocyte activation (66). Aliquots were then incubated with anti-Pbs21 antibody (1:500) for 1 hour, followed by anti-mouse IgG conjugated Alexa Fluor 594 (1:1,000) for another hour (65). Samples were centrifuged (3,000  $\times$  g for 3 minutes), pellets were resuspended in phosphate-buffered saline (PBS) and analyzed by flow cytometry (FACSCelesta, FACS Diva Software, BD Biosciences, San Jose, CA, USA) with 1 million events counted per experiment (66).

# In vitro toxicity assessment in HepG2 cells

HepG2 cell viability was assessed using the Cell Proliferation kit with trypan blue exclusion. Cells were seeded at  $2.5 \times 10^4$  per well in 96-well plates, incubated at  $37^{\circ}$ C in a humidified atmosphere of 5% CO<sub>2</sub>, and treated with 11 duplicate 1.6-fold serial dilutions of CB compounds (0.15–10 µg/mL) for 48 hours using a Biomek 4000 automated station. WR 288510-3 (IC<sub>50</sub> = 305.4 ng/mL) was used as a positive control. After incubation, a 1.5-mg/mL Cell Proliferation kit solution diluted in complete MEM medium was added to each well, followed by 1-hour dark incubation at 25°C. After aspiration of media and inhibitors, the plates were dried in a hood for 15 minutes, and acidified isopropyl alcohol was added to dissolve formazan dye crystals. The plates were then rotated for 15–30 minutes, and absorbance was determined using a Perkin Elmer Ensight plate reader.

# Synergy predictor

The MLSyPred tool (https://github.com/rcmi-igpd/MLSyPred) (67) predicted synergistic combinations between CB-61 and 85 FDA-approved antimalarial drugs. The tool analyzed the SMILES (Simplified Molecular Input Line Entry System) chemical formulas of the compounds and predicted synergy for each of the three models of *P. falciparum*.

# P. berghei blood-stage isobolograms

Antimalarial activity and IC<sub>50</sub> values of CB-61 and five antimalarial drugs were assessed using the previously described *in vitro* drug luminescence assay (14, 68). Blood-stage isobolograms were performed to confirm synergistic combinations between CB-61 and the five drugs, following established protocols (69). Thirty-two-fold IC<sub>50</sub> concentrations were used to obtain six concentration ranges for each drug combination, and then they were serially diluted five times (67). IC<sub>50</sub> scores for each drug alone were determined, and FIC<sub>50</sub> values (FIC<sub>50</sub> = IC<sub>50</sub> of each drug alone/IC<sub>50</sub> of each drug in combination) were calculated and plotted (70, 71). The Promega Luciferase Assay System Kit was used to measure mature schizonts' RLUs, and Giemsa blood smears confirmed the presence of schizonts (14).

#### Statistical analysis

Data were analyzed using GraphPad Prism Software 10.1.1. Dose–response curves were plotted, and  $IC_{50}$  values were calculated using a nonlinear regression function (14). Oocyst assays were analyzed using Kruskal-Wallis multiple comparisons with the Dunn post-test, and the chi-square test analyzed the oocyst prevalence (63). Gametocyte activation assays were analyzed with a one-way analysis of variance (ANOVA) using Dunnett's multiple comparison tests (19). Differences were considered significant at P < 0.05.

#### **ACKNOWLEDGMENTS**

We thank Daniel Bargieri and Richard Eastman for providing the *P. berghei* GIMO Ookluc line; Barbara Stokes and Daniel Watson for technical advice on isobolograms; Carmen Cadilla and Ricardo González-Mendez for expert advice with protein purification and statistical analysis, respectively; Jose G. Ortiz for helpful discussions; Roberto Díaz-González, Viviana González-Umpierre, Sergio Ramos-Varela, Dorianmarie Vargas-Franco, Jennifer Díaz-Rivera, María Del Mar Figueroa-Gispert, and Alexandra Torres for technical assistance; Susan Corey for critical and insightful manuscript revision.

This research was partially funded by the National Institute on Minority Health and Health Disparities RCMI Grant: U54MD007600, the National Institute of General Medicinal Sciences Research Training Initiative for Student Enhancement RISE Grant: 5R25GM061151-22 to A.M.R.Q., and the Intramural Research Program of the Division of

Intramural Research (Al001250-01), National Institute of Allergy and Infectious Diseases (NIAID), NIH to J.V.R.

This material has been reviewed by the Walter Reed Army Institute of Research. There is no objection to its presentation and/or publication. The opinions or assertions contained herein are the private views of the author and are not to be construed as official, or as reflecting true views of the Department of the Army or the Department of Defense.

Conceptualization: A.E.S., J.V.R., E.E.C.L., and A.R.; methodology: A.M.R.Q., A.E.S., E.E.C.L., J.V.R., A.R., Z.R.P., H.K., S.E.L., A.B.O., J.B., Y.G., K.K., and N.R.; software: A.M.R.Q. and K.K.; validation: A.M.R.Q., J.V.R., A.R., J.B., Z.R.P., and K.K.; formal analysis: A.M.R.Q., E.E.C.L., Z.R.P., S.E.L., J.B., K.K., N.R., J.V.R., H.K., Y.G., D.A.F., and A.B.O.; investigation: A.M.R.Q., E.E.C.L., S.E.L., K.K., N.R., Z.R.P., H.K., and J.B.; resources: A.M.R.Q., J.B., J.V.R., A.R., Y.G., and A.E.S.; writing—original draft preparation: A.M.R.Q.; writing—review and editing: A.E.S., A.M.R.Q., E.E.C.L., J.V.R., Z.P., H.K., A.B.O., J.B., D.A.F., A.R., K.K., A.R.L., and Y.G.; visualization: A.M.R.Q., Z.R.P., H.K., S.E.L., K.K., N.R., A.R., and J.V.R.; supervision: J.V.R. and A.E.S.; project administration: A.E.S.; funding acquisition: A.M.R.Q., J.V.R., A.R., and A.E.S. All authors have read and agreed to the published version of the manuscript.

#### **AUTHOR AFFILIATIONS**

<sup>1</sup>Department of Microbiology and Medical Zoology, University of Puerto Rico School of Medicine, San Juan, Puerto Rico

<sup>2</sup>Laboratory of Malaria and Vector Research, National Institute of Allergy and Infectious Diseases, National Institutes of Health, Rockville, Maryland, USA

<sup>3</sup>Center for Global Health and Diseases, Case Western Reserve University, Cleveland, Ohio, USA

<sup>4</sup>InterRayBio, LLC, Cleveland, Ohio, USA

<sup>5</sup>Department of Drug Discovery, Experimental Therapeutics Branch, Walter Reed Army Institute of Research, Silver Spring, Maryland, USA

<sup>6</sup>Department of Biochemistry, University of Puerto Rico School of Medicine, San Juan, Puerto Rico

<sup>7</sup>RCMI Program, Medical Science Campus, University of Puerto Rico, San Juan, Puerto Rico <sup>8</sup>Department of Pharmacology and Toxicology, University of Puerto Rico School of Medicine, San Juan, Puerto Rico

<sup>9</sup>Department of Microbiology and Immunology, Columbia University, New York, New York, USA

<sup>10</sup>Division of Infectious Diseases, Department of Medicine, Center for Malaria Therapeutics and Antimicrobial Resistance, Columbia University Medical Center, New York, New York, USA

## **AUTHOR ORCIDs**

Joel Vega-Rodríguez http://orcid.org/0000-0002-9576-0058 Adelfa E. Serrano http://orcid.org/0000-0001-5929-9973

#### **FUNDING**

Funder	Grant(s)	Author(s)
HHS   NIH   National Institute on Minority Health and Health Disparities (NIMHD)	U54MD007600	Adelfa E. Serrano
HHS   NIH   National Institute of General Medical Sciences (NIGMS)	5R25GM061151-22	Angélica M. Rosado-Quiñones
HHS   NIH   NIAID   Division of Intramural Research (DIR, NIAID)	Al001250-01	Joel Vega-Rodríguez

#### **AUTHOR CONTRIBUTIONS**

Angélica M. Rosado-Quiñones, Formal analysis, Funding acquisition, Investigation, Methodology, Resources, Software, Validation, Visualization, Writing - original draft, Writing - review and editing | Emilee E. Colón-Lorenzo, Formal analysis, Investigation, Methodology, Writing - review and editing | Zarna Rajeshkumar Pala, Formal analysis, Investigation, Methodology, Validation, Visualization, Writing - review and editing Jürgen Bosch, Formal analysis, Investigation, Methodology, Resources, Validation, Writing - review and editing | Karl Kudyba, Formal analysis, Investigation, Methodology, Software, Validation, Visualization, Writing - review and editing | Heather Kudyba, Formal analysis, Investigation, Methodology, Visualization, Writing - review and editing Susan E. Leed, Formal analysis, Investigation, Methodology, Visualization | Norma Roncal, Formal analysis, Investigation, Methodology, Visualization | Abel Baerga-Ortiz, Formal analysis, Methodology, Writing – review and editing | Abiel Roche-Lima, Writing - review and editing | Yamil Gerena, Formal analysis, Methodology, Resources, Writing - review and editing | David A. Fidock, Formal analysis, Writing - review and editing | Alison Roth, Conceptualization, Funding acquisition, Methodology, Resources, Validation, Visualization, Writing - review and editing | Joel Vega-Rodríguez, Conceptualization, Formal analysis, Funding acquisition, Methodology, Resources, Supervision, Validation, Visualization, Writing – review and editing | Adelfa E. Serrano, Conceptualization, Funding acquisition, Methodology, Project administration, Resources, Supervision, Writing – review and editing

#### **ETHICS APPROVAL**

Animal experiments were conducted with Swiss-CD1 female mice from Charles River Laboratories (Wilmington, MA, USA) in agreement with the Laboratory Animal Care and Use Guidelines (National Research Council) and the Public Health Service's Humane Laboratory Animal Care and Use Policy regulations. All mouse experiments were conducted at the AAALAC-accredited University of Puerto Rico Medical Sciences Campus under IACUC protocol 2480108. LMVR Insectary SOPs 203, 601, 604, 605, and 606 guidelines were followed for *Anopheles* mosquito infections. *Anopheles stephensi* and *Anopheles dirus* mosquitoes (49) were raised under standard laboratory conditions. Commercially obtained, anonymized human blood was used for parasite cultures and mosquito feeding. Donors provided informed consent under NIH protocol 99 CC-0168. Experiments at USAMM-AFRIMS, a fully accredited AAALAC institution, were reviewed and approved by the USAMD-AFRIMS IACUC and Animal Use Review Division (protocol PN22-10).

#### **ADDITIONAL FILES**

The following material is available online.

#### Supplemental Material

**Supplemental figures (AAC01643-23-s0001.pdf).** Figure S1 and S2. **Supplemental data (AAC01643-23-s0002.xlsx).** Tables S1 to S3.

# **REFERENCES**

- 1. WHO. 2022. World health statistics, p 1–177. World Health.
- Blasco B, Leroy D, Fidock DA. 2017. Antimalarial drug resistance: linking Plasmodium falciparum parasite biology to the clinic. Nat Med 23:917– 928. https://doi.org/10.1038/nm.4381
- Box ED, Box QT, Young MD. 1963. Chloroquine-resistant *Plasmodium falciparum* from Porto Velho, Brazil. Am J Trop Med Hyg 12:300–304. https://doi.org/10.4269/ajtmh.1963.12.300
- Han CM, Grimmond TR. 1976. Chloroquine resistance trials in Papua New Guinea. 1. Maprik and Popondetta areas. P N G Med J 19:236–242.
- Harinasuta T, Suntharasamai P, Viravan C. 1965. Chloroquine-resistant Falciparum malaria in Thailand. Lancet 2:657–660. https://doi.org/10. 1016/s0140-6736(65)90395-8
- Moore DV, Lanier JE. 1961. Observations on two *Plasmodium falciparum* infections with an abnormal response to chloroquine. Am J Trop Med Hyg 10:5–9. https://doi.org/10.4269/ajtmh.1961.10.5
- Young MD, Moore DV. 1961. Chloroquine resistance in *Plasmodium falciparum*. Am J Trop Med Hyg 10:317–320. https://doi.org/10.4269/ajtmh.1961.10.317

- Ashley EA, Dhorda M, Fairhurst RM, Amaratunga C, Lim P, Suon S, Sreng S, Anderson JM, Mao S, Sam B, et al. 2014. Spread of artemisinin resistance in *Plasmodium falciparum* malaria. N Engl J Med 371:411–423. https://doi.org/10.1056/NEJMoa1314981
- Dondorp AM, Nosten F, Yi P, Das D, Phyo AP, Tarning J, Lwin KM, Ariey F, Hanpithakpong W, Lee SJ, Ringwald P, Silamut K, Imwong M, Chotivanich K, Lim P, Herdman T, An SS, Yeung S, Singhasivanon P, Day NPJ, Lindegardh N, Socheat D, White NJ. 2009. Artemisinin resistance in Plasmodium falciparum malaria. N Engl J Med 361:455–467. https://doi. org/10.1056/NEJMoa0808859
- Noedl H, Socheat D, Satimai W. 2009. Artemisinin-resistant malaria in Asia. N Engl J Med 361:540–541. https://doi.org/10.1056/NEJMc0900231
- Noedl H, Se Y, Schaecher K, Smith BL, Socheat D, Fukuda M. 2008. Artemisinin resistance in Cambodia 1 (ARC1) study consortium. evidence of artemisinin-resistant malaria in western Cambodia. Artemisinin resistance in Cambodia 1 (ARC1) study consortium. N Engl J Med 359:2619–2620. https://doi.org/10.1056/NEJMc0805011
- Lindner SE, Miller JL, Kappe SHI. 2012. Malaria parasite pre-erythrocytic infection: preparation meets opportunity. Cell Microbiol 14:316–324. https://doi.org/10.1111/j.1462-5822.2011.01734.x
- Smith RC, Vega-Rodríguez J, Jacobs-Lorena M. 2014. The *Plasmodium* bottleneck: malaria parasite losses in the mosquito vector. Mem Inst Oswaldo Cruz 109:644–661. https://doi.org/10.1590/0074-0276130597
- Colón-Lorenzo EE, Colón-López DD, Vega-Rodríguez J, Dupin A, Fidock DA, Baerga-Ortiz A, Ortiz JG, Bosch J, Serrano AE. 2020. Structure-based screening of *Plasmodium berghei* glutathione S-transferase identifies CB-27 as a novel antiplasmodial compound. Front Pharmacol 11:246. https://doi.org/10.3389/fphar.2020.00246
- Deponte M, Becker K. 2005. Glutathione S-transferase from malarial parasites: structural and functional aspects. Methods Enzymol 401:241– 253. https://doi.org/10.1016/S0076-6879(05)01015-3
- Patzewitz EM, Wong EH, Müller S. 2012. Dissecting the role of glutathione biosynthesis in *Plasmodium falciparum*. Mol Microbiol 83:304– 318. https://doi.org/10.1111/j.1365-2958.2011.07933.x
- Johnson JD, Dennull RA, Gerena L, Lopez-Sanchez M, Roncal NE, Waters NC. 2007. Assessment and continued validation of the malaria SYBR green I-based fluorescence assay for use in malaria drug screening. Antimicrob Agents Chemother 51:1926–1933. https://doi.org/10.1128/ AAC.01607-06
- Pastrana-Mena R, Dinglasan RR, Franke-Fayard B, Vega-Rodríguez J, Fuentes-Caraballo M, Baerga-Ortiz A, Coppens I, Jacobs-Lorena M, Janse CJ, Serrano AE. 2010. Glutathione reductase-null malaria parasites have normal blood stage growth but arrest during development in the mosquito. J Biol Chem 285:27045–27056. https://doi.org/10.1074/jbc. M110.122275
- Wang Y, Jadhav A, Southal N, Huang R, Nguyen DT. 2010. A grid algorithm for high throughput fitting of dose-response curve data. Curr Chem Genomics 4:57–66. https://doi.org/10.2174/-1875397301004010057
- de Souza GE, Bueno RV, de Souza JO, Zanini CL, Cruz FC, Oliva G, Guido RVC, Aguiar ACC. 2019. Antiplasmodial profile of selected compounds from malaria box: in vitro evaluation, speed of action and drug combination studies. Malar J 18:447. https://doi.org/10.1186/s12936-019-3069-3
- Katsuno K, Burrows JN, Duncan K, Hooft van Huijsduijnen R, Kaneko T, Kita K, Mowbray CE, Schmatz D, Warner P, Slingsby BT. 2015. Hit and lead criteria in drug discovery for infectious diseases of the developing world. Nat Rev Drug Discov 14:751–758. https://doi.org/10.1038/nrd4683
- Roche-Lima A, Rosado-Quiñones AM, Feliu-Maldonado RA, Figueroa-Gispert MDM, Díaz-Rivera J, Díaz-González RG, Carrasquillo-Carrion K, Nieves BG, Colón-Lorenzo EE, Serrano AE. 2024. Antimalarial drug combination predictions using the machine learning synergy predictor (MLSyPred®) tool. Acta Parasitol. https://doi.org/10.1007/s11686-023-00765-z
- Watson DJ, Meyers PR, Acquah KS, Dziwornu GA, Barnett CB, Wiesner L. 2021. Discovery of novel cyclic ethers with synergistic antiplasmodial activity in combination with valinomycin. Molecules 26:7494. https://doi. org/10.3390/molecules26247494
- Vega-Rodríguez J, Franke-Fayard B, Dinglasan RR, Janse CJ, Pastrana-Mena R, Waters AP, Coppens I, Rodríguez-Orengo JF, Srinivasan P, Jacobs-Lorena M, Serrano AE. 2009. The glutathione biosynthetic

- pathway of *Plasmodium* is essential for mosquito transmission. PLoS Pathog 5:e1000302. https://doi.org/10.1371/journal.ppat.1000302
- Zhang M, Wang C, Otto TD, Oberstaller J, Liao X, Adapa SR, Udenze K, Bronner IF, Casandra D, Mayho M, Brown J, Li S, Swanson J, Rayner JC, Jiang RHY, Adams JH. 2018. Uncovering the essential genome of the human malaria parasite *Plasmodium falciparum* by saturation mutagenesis. Science 360:eaap7847. https://doi.org/10.1126/science.aap7847
- Kalászi A, Szisz D, Imre G, Polgár T. 2014. Screen3D: a novel fully flexible high-throughput shape-similarity search method. J Chem Inf Model 54:1036–1049. https://doi.org/10.1021/ci400620f
- Kumar A, Zhang KYJ. 2016. Application of shape similarity in pose selection and virtual screening in CSARdock2014 exercise. J Chem Inf Model 56:965–973. https://doi.org/10.1021/acs.jcim.5b00279
- Liang JW, Wang S, Wang MY, Li SL, Li WQ, Meng FH. 2019. Identification of novel PI3Kδ selective inhibitors by SVM-based multistage virtual screening and molecular dynamics simulations. Int J Mol Sci 20:1–13. https://doi.org/10.3390/ijms20236000
- Wei Y, Li J, Chen Z, Wang F, Huang W, Hong Z, Lin J. 2015. Multistage virtual screening and identification of novel HIV-1 protease inhibitors by integrating SVM, shape, pharmacophore and docking methods. Eur J Med Chem 101:409–418. https://doi.org/10.1016/j.ejmech.2015.06.054
- Ramírez D, Caballero J. 2016. Is it reliable to use common molecular docking methods for comparing the binding affinities of enantiomer pairs for their protein target?. Int J Mol Sci 17:1–15. https://doi.org/10. 3390/ijms17040525
- Liebau E, Dawood KF, Fabrini R, Fischer-Riepe L, Perbandt M, Stella L, Pedersen JZ, Bocedi A, Petrarca P, Federici G, Ricci G. 2009. Tetramerization and cooperativity in *Plasmodium falciparum* glutathione Stransferase are mediated by atypic loop 113-119. J Biol Chem 284:22133–22139. https://doi.org/10.1074/jbc.M109.015198
- Al-Qattan MN, Mordi MN, Mansor SM. 2016. Assembly of ligands interaction models for glutathione-S-transferases from *Plasmodium* falciparum, human and mouse using enzyme kinetics and molecular docking. Comput Biol Chem 64:237–249. https://doi.org/10.1016/j. compbiolchem.2016.07.007
- Orjih AU, Banyal HS, Chevli R, Fitch CD. 1981. Hemin lyses malaria parasites. Science 214:667–669. https://doi.org/10.1126/science. 7027441
- Grenoble DC, Drickamer HG. 1968. The effect of pressure on the oxidation state of iron. 3. Hemin and hematin. Proc Natl Acad Sci U S A 61:1177–1182. https://doi.org/10.1073/pnas.61.4.1177
- Ahmad R, Srivastava AK, Tripathi RP, Batra S, Walter RD. 2007. Synthesis and biological evaluation of potential modulators of malarial glutathione-S-transferase(S). J Enzyme Inhib Med Chem 22:327–342. https:// doi.org/10.1080/14756360601072676
- Harwaldt P, Rahlfs S, Becker K. 2002. Glutathione S-transferase of the malarial parasite *Plasmodium falciparum*: characterization of a potential drug target. Biol Chem 383:821–830. https://doi.org/10.1515/BC.2002. 086
- Hiller N, Fritz-Wolf K, Deponte M, Wende W, Zimmermann H, Becker K.
   2006. Plasmodium falciparum glutathione S -transferase-structural and mechanistic studies on ligand binding and enzyme inhibition. Protein Sci 15:281–289. https://doi.org/10.1110/ps.051891106
- 38. Colón-Lorenzo EE, Serrano AE, Nicholas HB, Wymore T, Ropelewski AJ, González-Méndez R. 2010. "The *Plasmodium* glutathione S-transferase: bioinformatics characterization and classification into the sigma class" Bioinforma 2010 Proc 1st Int Conf Bioinforma, p 173–180
- Valenciano AL, Gomez-Lorenzo MG, Vega-Rodríguez J, Adams JH, Roth A. 2022. *In vitro* models for human malaria: targeting the liver stage. Trends Parasitol 38:758–774. https://doi.org/10.1016/j.pt.2022.05.014
- Fontinha D, Moules I, Prudêncio M. 2020. Repurposing drugs to fight hepatic malaria parasites. Molecules 25:3409. https://doi.org/10.3390/ molecules25153409
- Flannery EL, Foquet L, Chuenchob V, Fishbaugher M, Billman Z, Navarro MJ, Betz W, Olsen TM, Lee J, Camargo N, Nguyen T, Schafer C, Sack BK, Wilson EM, Saunders J, Bial J, Campo B, Charman SA, Murphy SC, Phillips MA, Kappe SH, Mikolajczak SA. 2018. Assessing drug efficacy against *Plasmodium falciparum* liver stages *in vivo*. JCl Insight 3:1–12. https://doi.org/10.1172/jci.insight.92587
- Wampfler R, Hofmann NE, Karl S, Betuela I, Kinboro B, Lorry L, Silkey M, Robinson LJ, Mueller I, Felger I. 2017. Effects of liver-stage clearance by

- primaquine on gametocyte carriage of *Plasmodium vivax* and *P. falciparum*. PLoS Negl Trop Dis 11:e0005753. https://doi.org/10.1371/journal.pntd.0005753
- Llanos-Cuentas A, Lacerda MVG, Hien TT, Vélez ID, Namaik-Larp C, Chu CS, Villegas MF, Val F, Monteiro WM, Brito MAM, et al. 2019. Tafenoquine versus primaquine to prevent relapse of *Plasmodium vivax* malaria. N Engl J Med 380:229–241. https://doi.org/10.1056/NEJMoa1802537
- Recht J, Ashley EA, White NJ. 2018. Use of primaquine and glucose-6phosphate dehydrogenase deficiency testing: divergent policies and practices in malaria endemic countries. PLoS Negl Trop Dis 12:e0006230. https://doi.org/10.1371/journal.pntd.0006230
- Rodríguez-Hernández D, Vijayan K, Zigweid R, Fenwick MK, Sankaran B, Roobsoong W, Sattabongkot J, Glennon EKK, Myler PJ, Sunnerhagen P, Staker BL, Kaushansky A, Grøtli M. 2023. Identification of potent and selective N-myristoyltransferase inhibitors of *Plasmodium vivax* liver stage hypnozoites and schizonts. Nat Commun 14:5408. https://doi.org/ 10.1038/s41467-023-41119-7
- Maher SP, Bakowski MA, Vantaux A, Flannery EL, Andolina C, Gupta M, Antonova-Koch Y, Argomaniz M, Cabrera-Mora M, Campo B, et al. 2023. A drug repurposing approach reveals targetable epigenetic pathways in Plasmodium vivax hypnozoites. bioRxiv. https://doi.org/10.1101/2023.01. 31.526483
- 47. Page KM. 2016. Validation of early human dose prediction: a key metric for compound progression in drug discovery. Mol Pharm 13:609–620. https://doi.org/10.1021/acs.molpharmaceut.5b00840
- Chou TC. 2006. Theoretical basis, experimental design, and computerized simulation of synergism and antagonism in drug combination studies. Pharmacol Rev 58:621–681. https://doi.org/10.1124/pr.58.3.10
- Huang R, Pei L, Liu Q, Chen S, Dou H, Shu G, Yuan Z, Lin J, Peng G, Zhang W, Fu H. 2019. Isobologram analysis: a comprehensive review of methodology and current research. Front Pharmacol 10:1–12. https:// doi.org/10.3389/fphar.2019.01222
- Li X, Qin G, Yang Q, Chen L, Xie L. 2016. Biomolecular network-based synergistic drug combination discovery. Biomed Res Int 2016:8518945. https://doi.org/10.1155/2016/8518945
- Lell B, Kremsner PG. 2002. Clindamycin as an antimalarial drug: review of clinical trials. Antimicrob Agents Chemother 46:2315–2320. https://doi. org/10.1128/AAC.46.8.2315-2320.2002
- Le Bras J, Durand R. 2003. The mechanisms of resistance to antimalarial drugs in *Plasmodium falciparum*. Fundam Clin Pharmacol 17:147–153. https://doi.org/10.1046/j.1472-8206.2003.00164.x
- Feldmann AM, Ponnudurai T. 1989. Selection of anopheles stephensi for refractoriness and susceptibility to *Plasmodium falciparum*. Med Vet Entomol 3:41–52. https://doi.org/10.1111/j.1365-2915.1989.tb00473.x
- Spaccapelo R, Janse CJ, Caterbi S, Franke-Fayard B, Bonilla JA, Syphard LM, Di Cristina M, Dottorini T, Savarino A, Cassone A, Bistoni F, Waters AP, Dame JB, Crisanti A. 2010. Plasmepsin 4-deficient *Plasmodium* berghei are virulence attenuated and induce protective immunity against experimental malaria. Am J Pathol 176:205–217. https://doi.org/ 10.2353/ajpath.2010.090504
- Calit J, Dobrescu I, Gaitán XA, Borges MH, Ramos MS, Eastman RT, Bargieri DY. 2018. Screening the pathogen box for molecules active against *Plasmodium* sexual stages using a new nanoluciferase-based. Antimicrob Agents Chemother 62:1–9. https://doi.org/10.1128/AAC. 01053-18
- Alves E Silva TL, Radtke A, Balaban A, Pascini TV, Pala ZR, Roth A, Alvarenga PH, Jeong YJ, Olivas J, Ghosh AK, Bui H, Pybus BS, Sinnis P, Jacobs-Lorena M, Vega-Rodríguez J. 2021. The fibrinolytic system enables the onset of *Plasmodium* infection in the mosquito vector and the mammalian host. Sci Adv 7:1–16. https://doi.org/10.1126/sciadv. abe3362
- Grote A, Hiller K, Scheer M, Münch R, Nörtemann B, Hempel DC, Jahn D. 2005. JCat: a novel tool to adapt codon usage of a target gene to its potential expression host. Nucleic Acids Res 33:W526–W531. https://doi. org/10.1093/nar/gki376
- Plouffe D, Brinker A, McNamara C, Henson K, Kato N, Kuhen K, Nagle A, Adrián F, Matzen JT, Anderson P, Nam T-G, Gray NS, Chatterjee A, Janes J, Yan SF, Trager R, Caldwell JS, Schultz PG, Zhou Y, Winzeler EA. 2008. In

- silico activity profiling reveals the mechanism of action of antimalarials discovered in a high-throughput screen. Proc Natl Acad Sci U S A 105:9059–9064. https://doi.org/10.1073/pnas.0802982105
- Roth A, Adapa SR, Zhang M, Liao X, Saxena V, Goffe R, Li S, Ubalee R, Saggu GS, Pala ZR, Garg S, Davidson S, Jiang RHY, Adams JH. 2018. Unraveling the *Plasmodium vivax* sporozoite transcriptional journey from mosquito vector to human host. Sci Rep 8:12183. https://doi.org/ 10.1038/s41598-018-30713-1
- 60. Vanachayangkul P, Im-Erbsin R, Tungtaeng A, Kodchakorn C, Roth A, Adams J, Chaisatit C, Saingam P, Sciotti RJ, Reichard GA, Nolan CK, Pybus BS, Black CC, Lugo-Roman LA, Wegner MD, Smith PL, Wojnarski M, Vesely BA, Kobylinski KC. 2020. Safety, pharmacokinetics, and activity of high-dose Ivermectin and chloroquine against the liver stage of *Plasmodium cynomolgi* infection in rhesus macaques. Antimicrob Agents Chemother 64:e00741-20. https://doi.org/10.1128/AAC.00741-20
- Roth A, Maher SP, Conway AJ, Ubalee R, Chaumeau V, Andolina C, Kaba SA, Vantaux A, Bakowski MA, Thomson-Luque R, et al. 2018. A comprehensive model for assessment of liver stage therapies targeting *Plasmodium vivax* and *Plasmodium falciparum*. Nat Commun 9:1837. https://doi.org/10.1038/s41467-018-04221-9
- 62. Gupta DK, Dembele L, Voorberg-van der Wel A, Roma G, Yip A, Chuenchob V, Kangwanrangsan N, Ishino T, Vaughan AM, Kappe SH, Flannery EL, Sattabongkot J, Mikolajczak S, Bifani P, Kocken CH, Diagana TT. 2019. The *Plasmodium* liver-specific protein 2 (LISP2) is an early marker of liver stage development. Elife 8:1–21. https://doi.org/10.7554/eLife.43362
- Gural N, Mancio-Silva L, Miller AB, Galstian A, Butty VL, Levine SS, Patrapuvich R, Desai SP, Mikolajczak SA, Kappe SHI, Fleming HE, March S, Sattabongkot J, Bhatia SN. 2018. *In vitro* culture, drug sensitivity, and transcriptome of *Plasmodium vivax* hypnozoites. Cell Host Microbe 23:395–406. https://doi.org/10.1016/j.chom.2018.01.002
- 64. Vega-Rodríguez J, Ghosh AK, Kanzok SM, Dinglasan RR, Wang S, Bongio NJ, Kalume DE, Miura K, Long CA, Pandey A, Jacobs-Lorena M. 2014. Multiple pathways for *Plasmodium ookinete* invasion of the mosquito midgut. Proc Natl Acad Sci U S A 111:E492–500. https://doi.org/10.1073/pnas.1315517111
- Pascini TV, Jeong YJ, Huang W, Pala ZR, Sá JM, Wells MB, Kizito C, Sweeney B, Alves e Silva TL, Andrew DJ, Jacobs-Lorena M, Vega-Rodríguez J. 2022. Transgenic anopheles mosquitoes expressing human PAI-1 impair malaria transmission. Nat Commun 13:1–16. https://doi.org/ 10.1038/s41467-022-30606-y
- Pastrana-Mena R, Mathias DK, Delves M, Rajaram K, King JG, Yee R, Trucchi B, Verotta L, Dinglasan RR. 2016. A malaria transmission-blocking (+)-Usnic acid derivative prevents *Plasmodium zygote*-to-ookinete maturation in the mosquito Midgut. ACS Chem Biol 11:3461–3472. https://doi.org/10.1021/acschembio.6b00902
- Kadota K, Ishino T, Matsuyama T, Chinzei Y, Yuda M. 2004. Essential role
  of membrane-attack protein in malarial transmission to mosquito host.
  Proc Natl Acad Sci U S A 101:16310–16315. https://doi.org/10.1073/pnas.
  0406187101
- Winger LA, Tirawanchai N, Nicholas J, Carter HE, Smith JE, Sinden RE. 1988. Ookinete antigens of *Plasmodium berghei*. appearance on the zygote surface of an Mr 21 kD determinant identified by transmissionblocking monoclonal antibodies. Parasite Immunol 10:193–207. https:// doi.org/10.1111/j.1365-3024.1988.tb00214.x
- Vega-Rodriguez J, Perez-Barreto D, Ruiz-Reyes A, Jacobs-Lorena M. 2015.
   Targeting molecular interactions essential for *Plasmodium* sexual reproduction. Cell Microbiol 17:1594–1604. https://doi.org/10.1111/cmi. 12458
- Lin JW, Sajid M, Ramesar J, Khan SM, Janse CJ, Franke-Fayard B. 2013.
   Screening inhibitors of *P. berghei* blood stages using bioluminescent reporter parasites. Methods Mol Biol 923:507–522. https://doi.org/10. 1007/978-1-62703-026-7\_35
- 71. Fivelman QL, Adagu IS, Warhurst DC. 2004. Modified fixed-ratio isobologram method for studying *in vitro* interactions between atovaquone and proguanil or dihydroartemisinin against drug-resistant strains of *Plasmodium falciparum*. Antimicrob Agents Chemother 48:4097–4102. https://doi.org/10.1128/AAC.48.11.4097-4102.2004